

# 冈底斯成矿带西段则不吓铅锌矿床钾长花岗斑岩年代学、地球化学及地质意义

杜保峰<sup>1,2)</sup>, 何凯<sup>2)</sup>, 杨长青<sup>2)</sup>, 蔡志超<sup>2)</sup>, 鲁培庆<sup>2)</sup>, 耿爱宾<sup>2)</sup>

1) 中国地质大学(北京)地球科学与资源学院, 北京, 100083;  
2) 河南省地质调查院, 河南省金属矿产成矿地质过程与资源利用重点实验室, 郑州, 450001

**内容提要:** 则不吓铅锌矿床位于冈底斯成矿带西段, 西藏谢通门县境内, 矿区发育大量钾长花岗斑岩, 其与铅锌成矿存在密切联系。通过对其开展岩石学、LA-MC-ICP-MS 锆石 U-Pb 年代学和岩石地球化学研究, 探讨区内钾长花岗斑岩岩石成因、侵入时代及其与铅锌成矿之间的关系。岩石地球化学结果显示, 钾长花岗斑岩具高硅、富钾而贫镁特征, A/CNK 值介于 1.08~1.38 之间; REE 具有较明显中等负 Eu 异常, 总体呈现右倾的轻稀土富集特征, 微量元素富集 Rb、K、U、Th、Pb 等大离子亲石元素, 而 Ba、Sr 和 Nb、Ta、Ti、P 等高场强元素相对亏损。岩石地球化学研究表明钾长花岗斑岩属分异的 S 型花岗岩。锆石 U-Pb 测年结果显示, 钾长花岗斑岩侵位年龄为  $14.18 \pm 0.15$  Ma, 系中新世岩浆作用产物, 与印度—亚洲大陆碰撞后伸展背景下的引张构造有关, 并与冈底斯成矿带中新世大规模斑岩侵位时代和相关斑岩型铜(钼)矿化时代一致, 可能具有相同的成岩成矿环境, 这为在该成矿带西段寻找与斑岩有关的铅锌矿床提供了参考。

**关键词:** 锆石 U-Pb 测年; 地球化学; 钾长花岗斑岩; 中新世; 则不吓; 冈底斯成矿带

冈底斯成矿带位于拉萨地体中南部, 夹于雅鲁藏布江缝合带与狮泉河—纳木错蛇绿混杂岩带之间, 是我国西部重点成矿区带之一(黄瀚霄等, 2019)。近些年随着勘查和研究的不断深入, 在该带已成功发现驱龙、甲玛、冲江、邦铺、亚贵拉、蒙亚阿、纳如松多、龙玛拉等大型—超大型矿床(图 1), 显示冈底斯是一条资源潜力巨大的铜—多金属矿带(李光明等, 2006; 孟祥金等, 2007; 唐菊兴等, 2014)。关于该带的成岩—成矿年龄主要集中于 62~41 Ma、30~23 Ma 和 18~12 Ma 三个阶段(费光春等, 2010; 张松等, 2012; 赵晓燕等, 2013; 纪现华等, 2014; 黄勇等, 2015; 马旺等, 2020), 分别对应于印度—亚洲大陆主碰撞造山成矿、晚碰撞转换成矿和后碰撞伸展成矿时段(侯增谦等, 2006, 2012)。在该带东段发育的铅—锌—银矿化以矽卡岩型为主, 而西段发育的铅—锌—银矿化多以热液脉型矿床为主, 并有少量隐爆角砾岩型, 其中热液脉型矿体以脉状产于古生代或新生代地层中的构造破碎带内, 多与新生代侵入的花岗斑岩小岩体有关(臧文栓等, 2007; 李光明等, 2011; 唐菊兴等, 2016)。

西藏谢通门县则不吓铅锌矿床是冈底斯西段新发现的一受构造—岩浆活动控制的热液脉状铅—锌—多金属矿床(杜保峰等, 2019), 受限于矿床较低的勘查程度, 区内广泛侵位的钾长花岗斑岩脉侵入时代及形成环境、与铅—锌成矿之关系等方面的研究较为薄弱。因此, 本文通过对矿区钾长花岗斑岩开展岩石学、地球化学和锆石 U-Pb 年代学等研究, 探讨其成岩时代、形成环境及与铅—锌成矿的关系, 以资区域地质研究和矿产勘查参考。

## 1 地质概况及岩石学特征

则不吓铅锌矿床大地构造位置位于拉萨地体的南冈底斯火山—岩浆弧带北部, 北临隆格尔—工布江达断隆带(潘桂棠等, 2004)。区域出露地层主要为石炭系—二叠系及古近系, 其中古近系林子宗群大面积分布, 与下伏地层呈角度不整合接触, 由中酸性火山岩、火山碎屑岩夹沉积碎屑岩组成; 区域出露侵入岩主要为燕山期和喜马拉雅期花岗岩类, 并有较多小型斑岩体分布。区域构造线总体呈近东西向, 以线性复式褶皱、压扭性逆冲推覆构造为主; 北



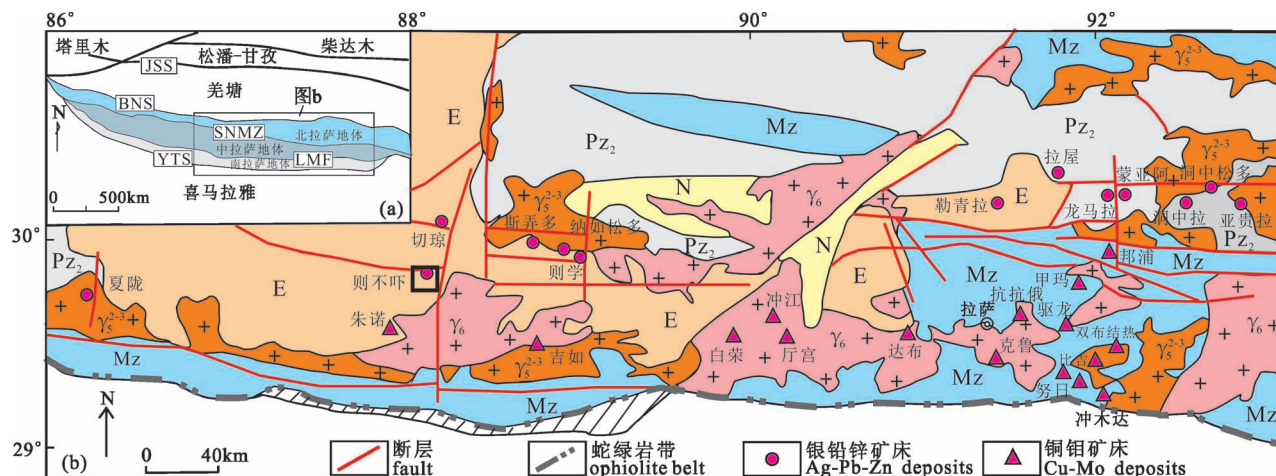


图 1 西藏冈底斯成矿带地质矿产简图(底图据臧文栓等,2007 修改)

Fig. 1 Sketch showing geological and mineral resources of Gangdese metallogenic belt

(modified after Zang Wenshuan et al., 2007&)

JSS—金沙江缝合带；BNS—班公湖—怒江缝合带；SNMZ—狮泉河—纳木错蛇绿混杂岩带；LMF—洛巴堆—米拉山断裂带；YTS—雅鲁

藏布江缝合带；N—新近系；E—古近系；Mz—中生界；Pz<sub>2</sub>—上古生界；γ<sub>6</sub>—喜马拉雅期花岗岩；γ<sub>5</sub><sup>2-3</sup>—燕山期花岗岩

JSS—Jinsha River suture zone; BNS—Bangong Lake—Nujiang River suture zone; SNMZ—Shiquanhe—Nam Lake ophiolite mélange zone; LMF—Luobadui—Mila Mountain fault zone; YTS—Yarlung River suture zone; N—Neogene; E—Paleogene; Mz—Mesozoic; Pz<sub>2</sub>—Upper Paleozoic; γ<sub>6</sub>—Himalayan granite; γ<sub>5</sub><sup>2-3</sup>—Yanshanian granite

东向及近南北向构造形成较晚,以发育张性构造为  
主要特征(臧文栓等,2007;赵晓燕等,  
2013)。

则不吓铅锌矿区出露地层主要为下  
二叠统昂杰组(P<sub>1</sub>a)、古近系林子宗群典  
中组(E<sub>1</sub>d)及第四系(Q)(图2)。昂杰组  
出露较多,主要岩性为石英砂岩、粉砂质  
板岩、泥质板岩;典中组广泛分布于矿区,  
主要岩性为安山质凝灰岩、英安质晶屑凝  
灰岩、流纹质(岩屑)晶屑凝灰岩和含角砾  
凝灰岩组成;第四系主要沿沟谷及河流两  
侧发育,以砂砾石堆积为主,为含泥砾石  
层、含砂砾石层。侵入岩主要为始新世似  
斑状黑云母二长花岗岩及钾长花岗斑岩  
出露;其中钾长花岗斑岩数量众多,广泛  
发育,其以岩脉、岩枝状呈NE—NNE向展  
布,少量呈近SN向(图3a)。矿区发育  
NNE—NE、近SN和NNW向三组脆性断  
裂,其中以NNE—NE向断裂较为发育,与  
成矿关系最为密切,其与NW向断层交汇  
部位严格控制了铅锌矿(化)体的展布。

矿区内地质矿产简图(图1)显示,已发现  
的7条铅锌矿(化)体呈不规则扁透镜状和  
脉状产出,均赋存于典中组NE—近SN向  
展布的断层破碎带内,且基本与相邻产出的  
钾长花岗斑岩走向一致,带内,且基本与相邻产出的钾长花岗斑岩走向一致,

带内,且基本与相邻产出的钾长花岗斑岩走向一致,

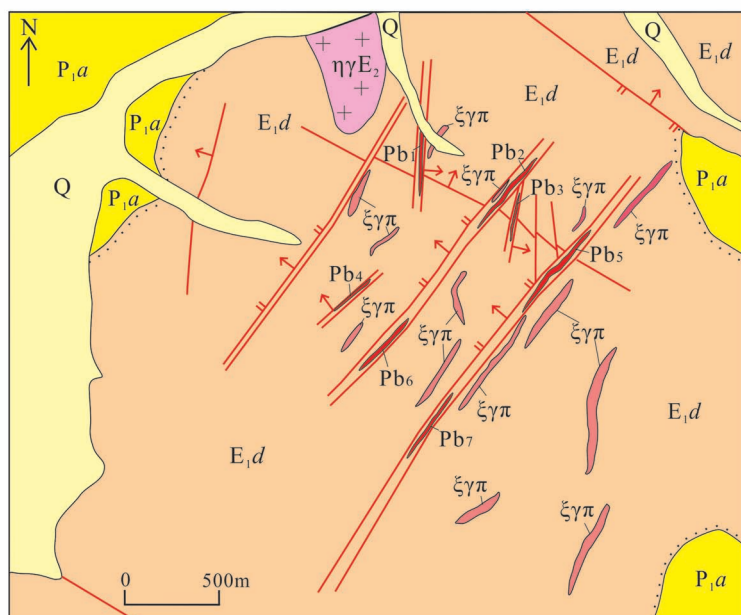


图 2 冈底斯成矿带西段则不吓铅锌矿床地质简图

Fig. 2 Simplified geological map of Zebuxia Pb—Zn deposit in  
western Gangdese metallgenic belt

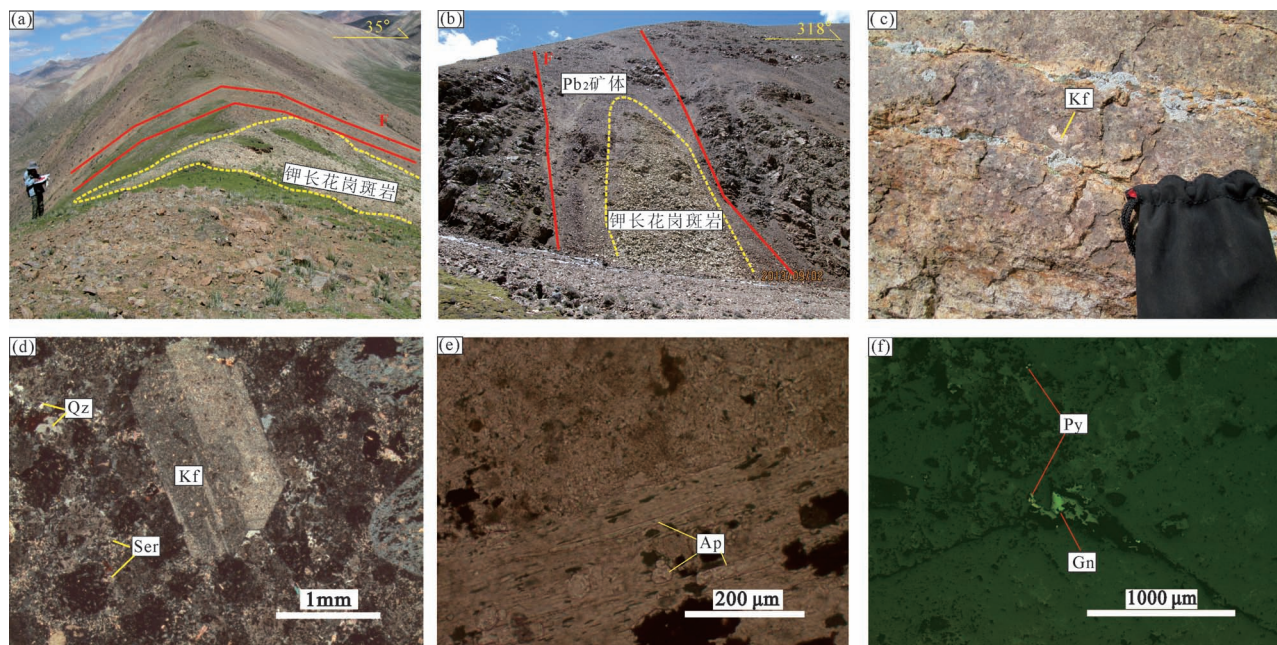


图 3 冈底斯成矿带西段则不吓矿床钾长花岗斑岩特征

Fig. 3 Characteristics of K-feldspar granite porphyries from the Zebuxia Pb—Zn deposit in western Gangdese metallgenetic belt  
 (a) 钾长花岗斑岩野外产出特征;(b) 断裂带内产出的钾长花岗斑岩和铅锌矿体;(c) 钾长花岗斑岩近照;(d) 钾长花岗斑岩显微照片及绢云母化;(e) 钾长花岗斑岩内副矿物磷灰石;(f) 钾长花岗斑岩内零星分布的黄铁矿和方铅矿;Kf—钾长石;Qz—石英;Ser—绢云母;Ap—磷灰石;Py—黄铁矿;Gn—方铅矿

(a) Field characteristics of K-feldspar granite porphyry; (b) K-feldspar granite porphyry and Pb—Zn orebody in fault zone; (c) close-up of K-feldspar granite porphyry; (d) micrograph of K-feldspar granite porphyry and its sericitization; (e) apatite of K-feldspar granite porphyry; (f) scattered pyrite and galena of K-feldspar granite porphyry. Kf—K-feldspar; Qz—quartz; Ap—apatite; Ser—sericite; Py—pyrite; Gn—galena

个别矿体与钾长花岗斑岩一起产于 NE 向断裂带内(图 3b),反映其可能受构造—岩浆活动的双重控制。各矿体 Pb 品位变化于 0.24%~19.42%,Zn 品位为 0.32%~5.46%,伴生 Ag 品位为  $2.7 \times 10^{-6}$ ~ $125 \times 10^{-6}$ 。矿石中主要金属矿物为方铅矿、黄铁矿和闪锌矿,局部见黄铜矿,表面和裂隙发育氧化矿物孔雀石和褐铁矿;方铅矿、黄铁矿、闪锌矿等主要以集合体形式呈浸染状、细脉状分布于碎裂凝灰岩中,少量呈致密块状。矿石具自形—半自形粒状结构、他形填隙结构、交代残余结构、脉状充填结构等,构造类型发育角砾状、细脉状和块状构造(杜保峰等,2019)。矿体围岩为典中组流纹质晶屑凝灰岩、含角砾凝灰岩及钾长花岗斑岩,靠近矿体的围岩中亦可见不同程度的黄铁矿化,局部可见零星方铅矿化。围岩蚀变发育硅化、绢云母化、高岭石化、碳酸盐化,铅锌矿化主要与硅化和绢云母化密切相关。

本次研究的钾长花岗斑岩均位于铅锌矿体周围,岩石呈灰红色,斑状结构(图 3c),基质呈微隐晶质结构,块状构造。斑晶矿物主要由钾长石(12%~

18%)、石英(3%~6%)和黑云母(1%~3%)等组成(图 3d)。其中钾长石斑晶,半自形—自形板状,粒径 0.6~4.5 mm,多数大于 1 mm,可见卡式双晶和微条纹;石英斑晶呈不规则状,部分呈浑圆状,个别发育溶蚀孔洞,粒径 0.3~1 mm;黑云母呈片状,发育绿泥石化。基质矿物主要由微隐晶长英质矿物(75%~82%)组成,副矿物主要为磁铁矿、锆石和磷灰石等(图 3e)。岩石多蚀变较强,表现为斑晶钾长石发育绢云母化、硅化和高岭土化,局部可见黄铁矿化和零星方铅矿化沿长石边缘分布(图 3f)。

## 2 样品及分析方法

用于 U-Pb 测年的 1 件样品(ZB/2)采自矿区 Pb<sub>5</sub> 矿体边部的钾长花岗斑岩内。锆石的样品破碎及挑选由河北廊坊区域地质矿产研究所实验室完成。室内将样品粉碎至 120 目以下,后用磁法和重力方法挑选,再在双目镜下挑选用于测年的锆石。将待测试的锆石颗粒采用环氧树脂固定,之后抛磨至锆石核部露出,最后对待测锆石进行镜下透射光、

反射光和阴极发光(CL)照相,锆石制靶和照相均在北京锆年领航科技有限公司完成。样品测年工作在天津地质矿产研究所同位素实验室完成,采用 LA-MC-ICP-MS 进行锆石 U-Pb 定年测试,ICP-MS 为 Agilent 7500a,分析采用直径为  $35 \mu\text{m}$  的激光束斑,剥蚀物质的载气为氦气,分析流程详见耿建珍等(2012),采用 Glitter4.0 软件对同位素比值等数据处理,普通铅校正则使用 Anderson(2002)的方法,并通过 Isoplot3.0 程序进行锆石谐和图绘制。

钾长花岗斑岩样品的主量-稀土-微量元素的配套分析由西南冶金地质测试中心完成,选择其中较弱蚀变的 5 件样品进行测试。对样品清洗烘干,在保证无污染后粉碎至 200 目。采用 X 射线荧光熔片法(XRF)测定主量元素,分析相对误差小于 1%,而微量元素和稀土元素分别采用电感耦合等离子质谱仪(ICP-MS)和电感耦合等离子体原子发射光谱法(ICP-AES)完成,分析相对误差小于 5%。

### 3 测试结果

#### 3.1 岩石地球化学特征

##### 3.1.1 主量元素特征

5 件钾长花岗斑岩样品的  $\text{SiO}_2$  含量为 69.86%~73.62%, $\text{Al}_2\text{O}_3$  为 13.82%~14.14%, $\text{K}_2\text{O} + \text{Na}_2\text{O}$  为 7.32%~8.69%(表 1),其中  $\text{K}_2\text{O}$  的含量 6.22%~6.78%,明显大于  $\text{Na}_2\text{O}$ (含量为 1.0%~2.41%),且  $\text{K}_2\text{O}/\text{Na}_2\text{O}$  值为 2.61~6.32;  $\text{TiFeO}$  (1.28%~1.87%), $\text{CaO}$  (0.76%~1.78%), $\text{MgO}$  (0.23%~

0.29%) 和  $\text{TiO}_2$  (0.22%~0.31%) 含量较低,钾长花岗斑岩总体具高硅、富钾而贫镁特征。岩石里特曼指数  $\sigma$  值介于 1.73~2.68 之间,均小于 3.3,显示出钙碱性岩浆岩的特征,在  $\text{SiO}_2-\text{K}_2\text{O}$  图(图 4a)中样品点多落在钾玄岩系列岩石区域。 $\text{A/CNK}$  值介于 1.08~1.38 之间(平均值 1.22),CIPW 标准中均出现了刚玉分子(1.27%~3.94%),无透辉石,基本属强过铝质,且在  $\text{A/CNK}-\text{A/NK}$  图解(图 4b)中均落入过铝质花岗岩区域。岩石分异指数( $DI$ )为 86.41~90.23,显示岩浆分异程度较高。

##### 3.1.2 稀土和微量元素特征

则不吓钾长花岗斑岩稀土元素总含量在  $223.0 \times 10^{-6}$ ~ $312.9 \times 10^{-6}$  之间(表 1),轻、重稀土元素比值(LREE/HREE)为 19.9~21.7, $(\text{La/Yb})_{\text{N}}$  值为 27.0~34.1,反映轻、重稀土元素发生较显著的分异;在稀土元素球粒陨石标准化配分模式图中呈现向右倾斜显著的趋势(图 5a),表明轻稀土富集而重稀土亏损,且均具有较明显的中等负 Eu 异常( $\delta\text{Eu}=0.49\sim0.60$ ),暗示岩浆形成过程中可能存在钾长石的分离结晶作用或者源区部分熔融时有斜长石的残留。钾长花岗斑岩富集 Rb、K、U、Th、Pb 等大离子亲石元素,而 Ba、Sr 和 Nb、Ta、Ti、P 等高场强元素则显示相对亏损;在微量元素原始地幔标准化蛛网图(图 5b)中,呈现出显著的 Rb、U、Th 等元素正异常和 Ba、Sr、Nb、Ti、P 等元素的负异常。

##### 3.2 锆石 U-Pb 年代学

则不吓钾长花岗斑岩样品 ZB/2 的锆石多数为

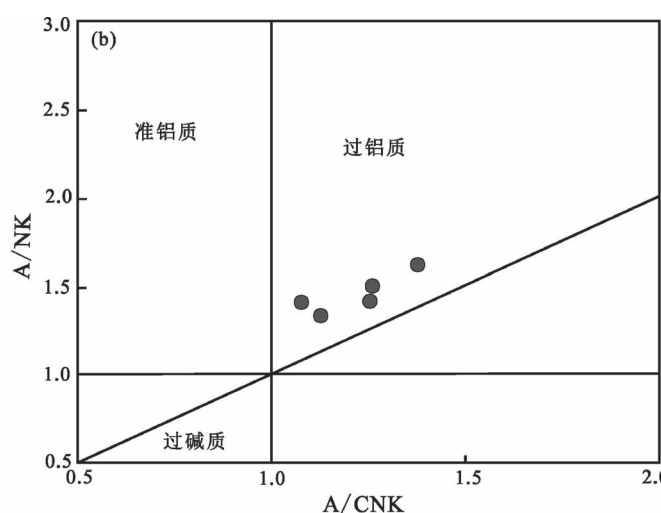
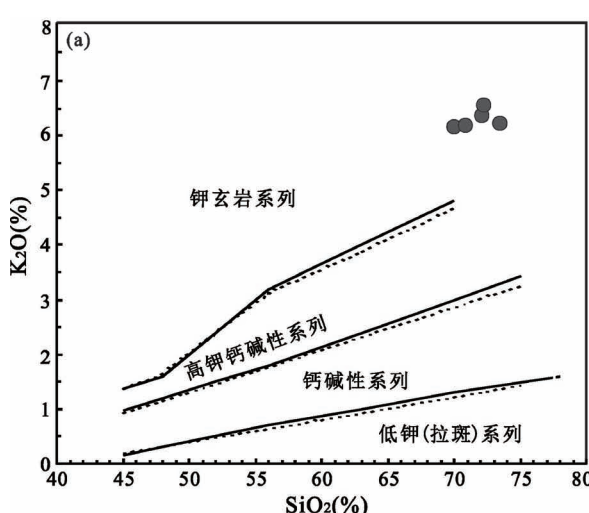


图 4 冈底斯成矿带西段则不吓矿床钾长花岗斑岩  $\text{SiO}_2-\text{K}_2\text{O}$ (a) 和  $\text{A/CNK}-\text{A/NK}$ (b) 判别图解

Fig. 4  $\text{SiO}_2-\text{K}_2\text{O}$  diagram (a) and  $\text{A/CNK}-\text{A/NK}$  diagram(b) of K-feldspar granite porphyries from the Zebuxia deposit in western Gangdese metallgenic belt

表1 冈底斯成矿带西段则不吓铅锌矿床钾长花岗斑岩主量元素(%)、微量元素和稀土元素( $\times 10^{-6}$ )分析结果  
Table1 Analysis results of major elements (%), Trace elements and REE ( $\times 10^{-6}$ ) of K-feldspar granite porphyries in Zebuxia Pb—Zn deposit, western Gangdese metallogenetic belt

样品号	ZB2-01	ZB2-02	ZB2-03	ZB2-04	ZB2-05	样品号	ZB2-01	ZB2-02	ZB2-03	ZB2-04	ZB2-05
SiO <sub>2</sub>	73.62	72.19	69.86	72.10	70.81	Ho	0.52	0.43	0.58	0.53	0.53
Al <sub>2</sub> O <sub>3</sub>	13.82	14.05	14.42	14.33	14.47	Er	1.62	1.33	1.84	1.61	1.62
Fe <sub>2</sub> O <sub>3</sub>	1.02	1.44	1.77	1.46	1.77	Tm	0.27	0.21	0.3	0.26	0.26
FeO	0.37	0.26	0.28	0.31	0.24	Yb	1.65	1.29	1.92	1.64	1.66
CaO	0.85	1.02	1.78	0.76	1.14	Lu	0.29	0.23	0.3	0.27	0.27
MgO	0.26	0.25	0.29	0.24	0.23	Y	16.4	12.6	18.6	16.1	15.8
K <sub>2</sub> O	6.32	6.78	6.22	6.53	6.28	$\Sigma$ REE	281.02	223.02	298.26	296.50	312.88
Na <sub>2</sub> O	1.00	1.19	2.08	1.81	2.41	LREE	268.36	212.36	283.35	283.03	299.10
TiO <sub>2</sub>	0.22	0.27	0.32	0.28	0.31	HREE	12.66	10.66	14.91	13.47	13.78
P <sub>2</sub> O <sub>5</sub>	0.04	0.07	0.11	0.07	0.10	LREE/HREE	21.20	19.92	19.00	21.01	21.71
MnO	0.04	0.04	0.06	0.04	0.05	(La/Yb) <sub>N</sub>	32.17	29.80	27.01	32.72	34.14
烧失量	2.26	2.23	2.62	1.90	1.97	$\delta$ Eu	0.49	0.60	0.59	0.55	0.56
总量	99.81	99.80	99.81	99.83	99.78	$\delta$ Ce	0.88	0.93	0.94	0.91	0.92
A/NK	1.63	1.51	1.42	1.43	1.34	Rb	392	402	390	398	383
A/CNK	1.38	1.26	1.08	1.25	1.13	Ba	355	582	610	522	628
DI	89.18	88.92	86.41	90.23	89.33	Th	120	112	108	114	115
$\sigma$	1.73	2.15	2.52	2.37	2.68	U	20	21	21.6	20	19.8
La	74	53.6	72.3	74.8	79	Ta	3.01	3.09	2.76	2.93	2.95
Ce	125	100	134	133	142	Nb	20	20	19	19.4	20.6
Pr	14.4	11.8	15.4	15.4	16.1	Sr	81.5	116	173	150	183
Nd	47.6	40.2	52.8	51.5	53.3	Zr	214	238	243	234	252
Sm	6.42	5.75	7.52	7.15	7.46	Hf	7.70	7.63	7.80	7.82	7.96
Eu	0.94	1.01	1.33	1.18	1.24	V	41.6	41.6	46.8	42.2	45.3
Gd	4.97	4.29	5.9	5.55	5.76	Sc	4.98	7.03	4.30	3.22	5.70
Tb	0.64	0.55	0.76	0.69	0.71	Pb	28.1	50.6	41.8	49.5	42.8
Dy	2.7	2.33	3.31	2.92	2.97						

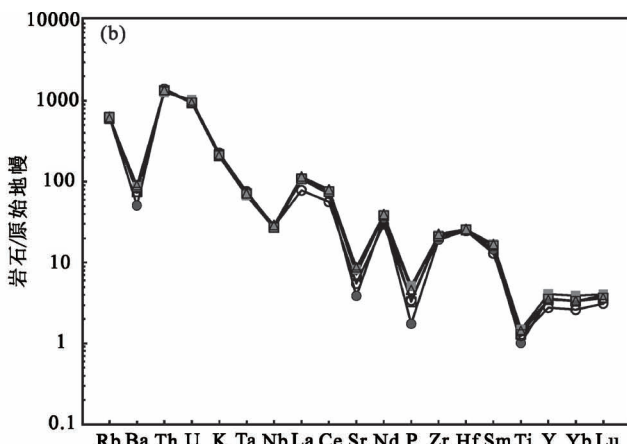
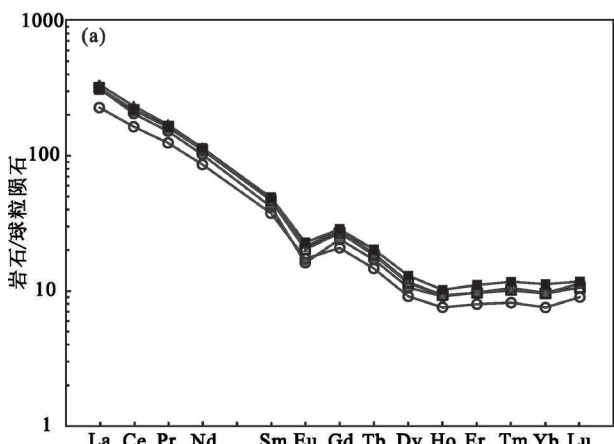


图5 冈底斯成矿带西段则不吓矿床钾长花岗斑岩稀土配分模式图(a)和微量元素蛛网图(b)  
(球粒陨石及原始地幔标准化值据 Sun and McDonough, 1989)

Fig. 5 Chondrite-normalized REE distribution patterns (a) and primitive mantle-normalized trace element spider patterns (b) for K-feldspar granite porphyries from the Zebuxia deposit in western Gangdese metallgenetic belt (The chondrite data and primitive mantle data for normalization after Sun and McDonough, 1989)

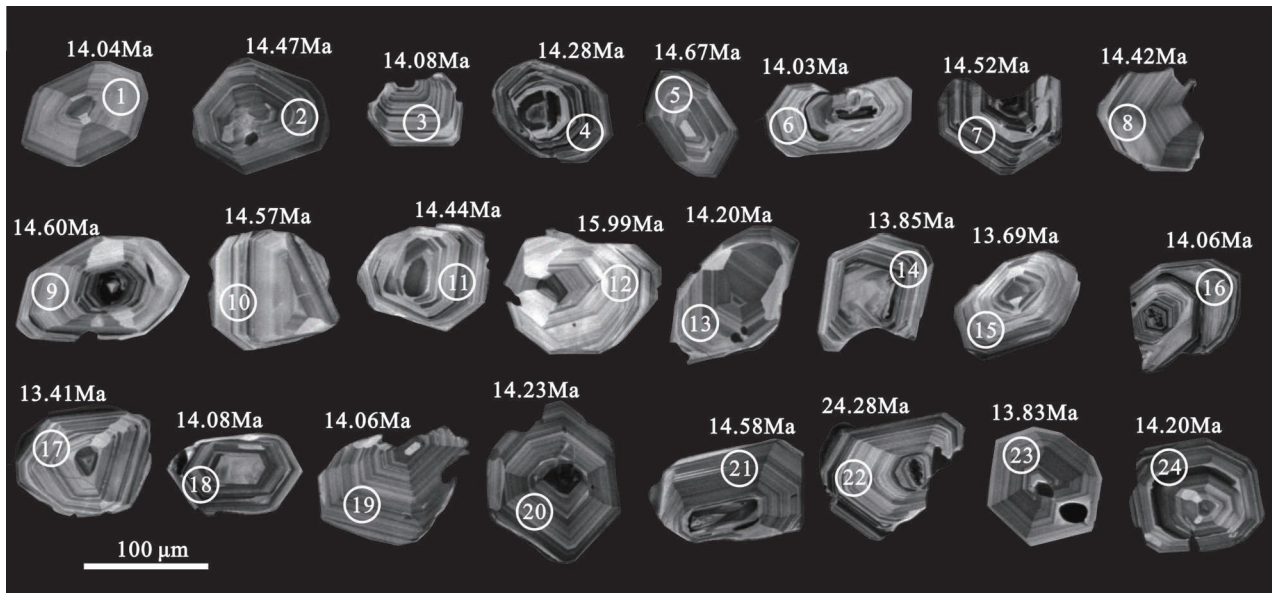


图 6 冈底斯成矿带西段则不吓矿床钾长花岗斑岩锆石阴极发光图

Fig. 6 Cathodoluminescence images from zircon grains of K-feldspar granite porphyry from the Zebuxia deposit in western Gangdese metallgenetic belt

浅黄色,次为无色,呈自形短柱状或长柱状、粒状,粒径长度在 70~200 mm 之间,长宽比大致为 1:1~3:1,阴极发光(CL)图像显示锆石多具清晰且均一的岩浆振荡环带(图 6),其边部或晶体内部常见港湾状溶蚀,可能为浅成—超浅成侵位造成的溶蚀。本次选择对 24 颗韵律环带明显的岩浆锆石进行了 U—Th—Pb 同位素分析。分析结果显示,锆石的 Th 与 U 含量变化较大,分别为  $383 \times 10^{-6}$ ~ $1586 \times 10^{-6}$  和  $394 \times 10^{-6}$ ~ $1864 \times 10^{-6}$ (表 2),且二者呈正相关关系,对应的 Th/U 值在 0.49~1.76 之间,与岩浆锆石 Th/U 值(大于 0.4)一致(Hoskin and Black, 2000; Griffin et al., 2004)。锆石 CL 图像显示具有清晰岩浆生长的韵律环带,这些特征均显示钾长花岗斑岩中锆石为典型的岩浆成因锆石(Hoskin and Schaltegger, 2003; Belousova et al., 2002; Moeller et al., 2003; 吴元保等,2004; 薛传东等,2010)。

锆石 U-Pb 测年结果显示(表 2),除去异常稍偏高的 2 个测点(12、22 号)年龄值,在 U-Pb 年龄谐和图中 22 个分析点均分布于谐和线上(图 7),表现出良好的谐和性,说明锆石形成之后的 U-Pb 同位素

体系是封闭的,基本无 U 或 Pb 同位素的丢失或加入。22 个锆石测点的  $n(^{206}\text{Pb})/n(^{238}\text{U})$  年龄范围在 13.69~14.67 Ma 之间,其加权平均年龄值为  $14.18 \pm 0.15$  Ma(95% 可信度, MSWD = 2.2,  $n = 22$ ),代表

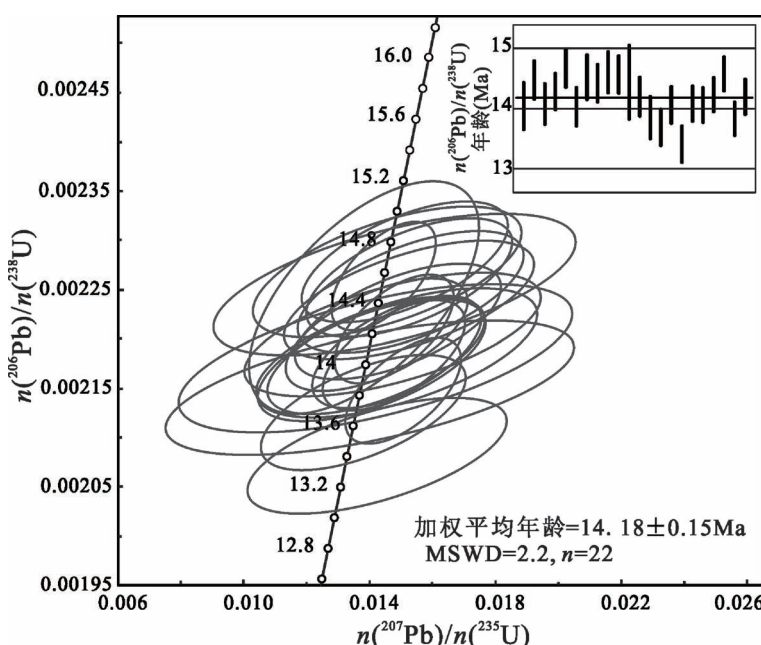


图 7 冈底斯成矿带西段则不吓矿床钾长花岗斑岩锆石 U-Pb 年龄谐和图

Fig. 7 U-Pb age concordia plots from zircon grains of K-feldspar granite porphyry from the Zebuxia deposit in western Gangdese metallgenetic belt

表 2 冈底斯成矿带西段则不吓铅锌矿床钾长花岗斑岩 LA-MC-ICP-MS 锆石 U-Pb 年龄测试结果

Table 2 LA-MC-ICP-MS zircon U-Pb isotopic data of K-feldspar granite porphyry in Zebuxia Pb-Zn deposit, western Gangdese metallogenic belt

测点号	元素含量( $\times 10^{-6}$ )			同位素比值						同位素年龄(Ma)				
	Pb	Th	U	Th/U			$n(^{206}\text{Pb})/n(^{238}\text{U})$			$n(^{207}\text{Pb})/n(^{235}\text{U})$			$n(^{207}\text{Pb})/n(^{238}\text{U})$	
				测值	$1\sigma$	测值	$1\sigma$	测值	$1\sigma$	测值	$1\sigma$	测值	$1\sigma$	
1	1.67	393	734	0.53	0.00218	0.00003	0.01419	0.00256	0.04720	0.00896	14.04	0.20	14.31	2.58
2	2.40	648	953	0.68	0.00225	0.00003	0.01531	0.00147	0.04940	0.00483	14.47	0.16	15.43	1.48
3	2.10	643	864	0.74	0.00219	0.00003	0.01487	0.00183	0.04933	0.00612	14.08	0.17	14.99	1.84
4	2.62	776	1044	0.74	0.00222	0.00002	0.01491	0.00134	0.04875	0.00438	14.28	0.15	15.03	1.35
5	3.05	936	1153	0.81	0.00228	0.00003	0.01513	0.00134	0.04815	0.00421	14.67	0.16	15.24	1.35
6	2.32	591	974	0.61	0.00218	0.00003	0.01407	0.00148	0.04685	0.00503	14.03	0.16	14.19	1.49
7	1.99	389	797	0.49	0.00226	0.00003	0.01480	0.00235	0.04759	0.00764	14.52	0.19	14.92	2.37
8	2.20	623	880	0.71	0.00224	0.00002	0.01526	0.00163	0.04941	0.00535	14.42	0.16	15.38	1.64
9	2.15	550	859	0.64	0.00227	0.00003	0.01457	0.00175	0.04658	0.00561	14.60	0.17	14.68	1.76
10	2.45	718	970	0.74	0.00226	0.00002	0.01527	0.00134	0.04894	0.00427	14.57	0.16	15.38	1.35
11	1.36	637	545	1.17	0.00224	0.00005	0.01383	0.00149	0.04473	0.00474	14.44	0.31	13.94	1.51
12	1.49	321	554	0.58	0.00248	0.00004	0.01671	0.00271	0.04880	0.00791	15.99	0.26	16.83	2.73
13	3.82	1586	1438	1.10	0.00220	0.00003	0.01474	0.00193	0.04848	0.00636	14.20	0.16	14.85	1.94
14	2.15	681	891	0.76	0.00215	0.00003	0.01401	0.00265	0.04726	0.00912	13.85	0.18	14.13	2.68
15	2.76	952	1115	0.85	0.00213	0.00002	0.01380	0.00133	0.04710	0.00455	13.69	0.15	13.92	1.34
16	2.59	814	1019	0.80	0.00218	0.00002	0.01421	0.00141	0.04720	0.00473	14.06	0.16	14.33	1.42
17	2.56	383	1209	0.32	0.00208	0.00002	0.01424	0.00169	0.04963	0.00595	13.41	0.15	14.36	1.70
18	3.42	1373	1251	1.10	0.00219	0.00002	0.01487	0.00110	0.04931	0.00361	14.08	0.15	14.99	1.11
19	3.10	873	1248	0.70	0.00218	0.00002	0.01478	0.00092	0.04909	0.00305	14.06	0.15	14.90	0.93
20	4.20	128	2044	0.06	0.00221	0.00002	0.01479	0.00077	0.04852	0.00250	14.23	0.14	14.90	0.78
21	8.48	4218	2401	1.76	0.00226	0.00002	0.01445	0.00068	0.04629	0.00212	14.58	0.14	14.57	0.68
22	1.88	408	394	1.04	0.00377	0.00005	0.02455	0.00394	0.04719	0.00793	24.28	0.34	24.63	3.96
23	4.50	1221	1864	0.66	0.00215	0.00002	0.01507	0.00075	0.05090	0.00254	13.83	0.14	15.19	0.76
24	2.92	665	1175	0.57	0.00220	0.00002	0.01423	0.00118	0.04682	0.00393	14.20	0.15	14.35	1.19

钾长花岗斑岩的冷却结晶年龄,表明其形成于中新世。

## 4 讨论及地质意义

### 4.1 岩石成因

目前花岗岩成因类型通过特征矿物和微量元素来判定已有大量文献论述。通常将含铝指数用来区分 I型和 S型花岗岩,I型花岗岩的 A/CNK 通常小于 1.1,而 S型花岗岩的 A/CNK 则往往大于 1.1 (Chappell, 1992),则不吓钾长花岗斑岩属富硅过铝质花岗岩,A/CNK 为 1.08~1.38,平均值 1.22,且刚玉分子含量>1% (1.27%~3.94%),具有 S型花岗岩特征。在  $K_2O-Na_2O$  图解中(图 8a),所有样品均位于 S型花岗岩范围之内;微量元素 Rb— $P_2O_5$  相关性趋势图解显示(图 8b),则不吓钾长花岗斑岩明显具有 S型花岗岩的特征;另外其 Rb/Sr 比值为 2.1~4.8,远大于 0.9,亦符合 S型花岗岩特征(董旭舟等,2014)。

则不吓钾长花岗斑岩富集 Rb、K、U、Th、Pb 等大离子亲石元素,而 Ba、Sr 和 Nb、Ta、Ti、P 等高场强元素呈现相对亏损,这些特征反映其形成过程中应存在大量地壳物质的混染。赵振华等(2008)研究表明 C<sub>I</sub>型球粒陨石 Nb/Ta 值为 17.3~17.6,大陆地壳的 Nb/Ta 值却相对偏低(10~14),则不吓钾长花岗斑岩 Nb/Ta 值为 8.4~10.1,比较接近大陆地壳,而 Zr/Hf 值 27.8~31.6(平均 30.3)亦接近大陆地壳平均值(33),反映以壳源为主;在 (La/Yb)<sub>N</sub>—Eu/Eu<sup>\*</sup> 图解上(图 8c),投点主要位于靠近壳幔型的壳型范围内,指示其主体具有地壳物质源区的特征,可能有地幔物质的少量加入。岩石 CaO/ $Na_2O$  值(0.42~0.86,平均 0.69)>0.3,与地壳的变砂岩源区相近,在 A/MF—C/MF 源岩判别图解(Alther et al., 2000)上(图 8d),样品投点主要落入变质砂岩部分熔融区域内,也反映其成因主要为地壳部分熔融。

钾长花岗斑岩样品在 TFeO/MgO—(Zr+Y+Ce+Nb)图解(whalen et al., 1987)上显示其为分异的花岗岩(图 8e);在 Bouseily and Sokkary(1975)提出的用于判别普通花岗岩和高分异花岗岩的 Rb—Ba—Sr 图中(图 8f),钾长花岗斑岩样品全部落入高分异型的区间。岩石中副矿物含有磷灰石,锆石中 U、Th 含量较高,全岩 Zr/Hf 值大于 25 而小于 55,属中等分异花岗岩(吴福元等,2017)。另外,钾长花岗斑岩本身分异程度较高(分异指数 DI 为 86.41~

90.23),且稀土配分曲线具较明显的中等负 Eu 异常,同样指示其发生了相对较强的结晶分异作用。上述综合判别指示则不吓钾长花岗斑岩应为地壳物质发生部分熔融形成的岩浆,期间可能有少量幔源物质加入,后经结晶分异演化形成的 S型花岗岩。

### 4.2 成岩构造环境

中新世,随着俯冲的印度大陆地壳边缘的岩石圈板片断离 (Miller et al., 1999; Maheo et al., 2002),深部软流圈物质沿断离板片窗上涌,诱发了亚欧大陆岩石圈地幔熔融。之后形成的幔源岩浆上侵并加热增厚的下地壳物质而发生壳—幔岩浆混合 (Hou Zengqian et al., 2009),在东西向伸展构造背景下形成了冈底斯带一系列钾质钙碱性熔岩、超钾质—钾质岩浆事件,以及数量众多的含矿斑岩体及中新世大规模成矿事件(曲晓明等, 2002; Hou Zengqian et al., 2004; 赵志丹等, 2006)。

本次钾长花岗斑岩的侵位年龄为  $14.2 \pm 0.2$  Ma,指示则不吓矿区广泛分布的钾长花岗斑岩应属中新世构造—岩浆活动的产物。在 (Y+Nb)—Rb 构造环境判别图解(图 9a)上,则不吓钾长花岗斑岩数据点均投于后碰撞花岗岩区域 (Pearce, 1996; Forster et al., 1997);(Rb/30)—Hf—(Ta×3)判别图解(图 9b)进一步确定钾长花岗斑岩投影于同碰撞花岗岩与碰撞晚期—碰撞后花岗岩交界处 (Harris et al., 1986),但主体偏向后者,具有后碰撞花岗岩的特征。Sylvester(1998)认为绝大多数与碰撞有关的强过铝质花岗岩都是“碰撞后”的,而则不吓钾长花岗斑岩为钾玄岩系列的强过铝质花岗岩,且钾玄质花岗岩可以形成于板块碰撞汇集后的松弛或局部伸展阶段 (Barbarin, 1999),表明其形成于碰撞后的张性构造环境。因此,则不吓钾长花岗斑岩应与冈底斯带同时代含矿斑岩体构造环境相似,可能与印度—亚洲大陆碰撞后伸展背景下的引张构造有关。

### 4.3 与铅锌成矿的关系

则不吓钾长花岗斑岩在各铅—锌矿体附近均有侵位,少量钾长花岗斑岩赋存于含矿构造带内,走向与矿体大体一致,其内局部有星点状黄铁矿化和方铅矿化沿长石边缘分布,且与铅锌矿体紧邻的钾长花岗斑岩也发育不同程度的绢云母化和硅化,反映铅—锌矿体的形成应与钾长花岗斑岩的侵位存在较密切的成因联系,其应属受构造—岩浆活动控制的热液矿床。近年来的研究表明,与金属成矿有关的花岗岩多具高 K、高的氧逸度和富含挥发分特征 (Sillitoe, 1997; Kelley and Ludington, 2002; 赵振华

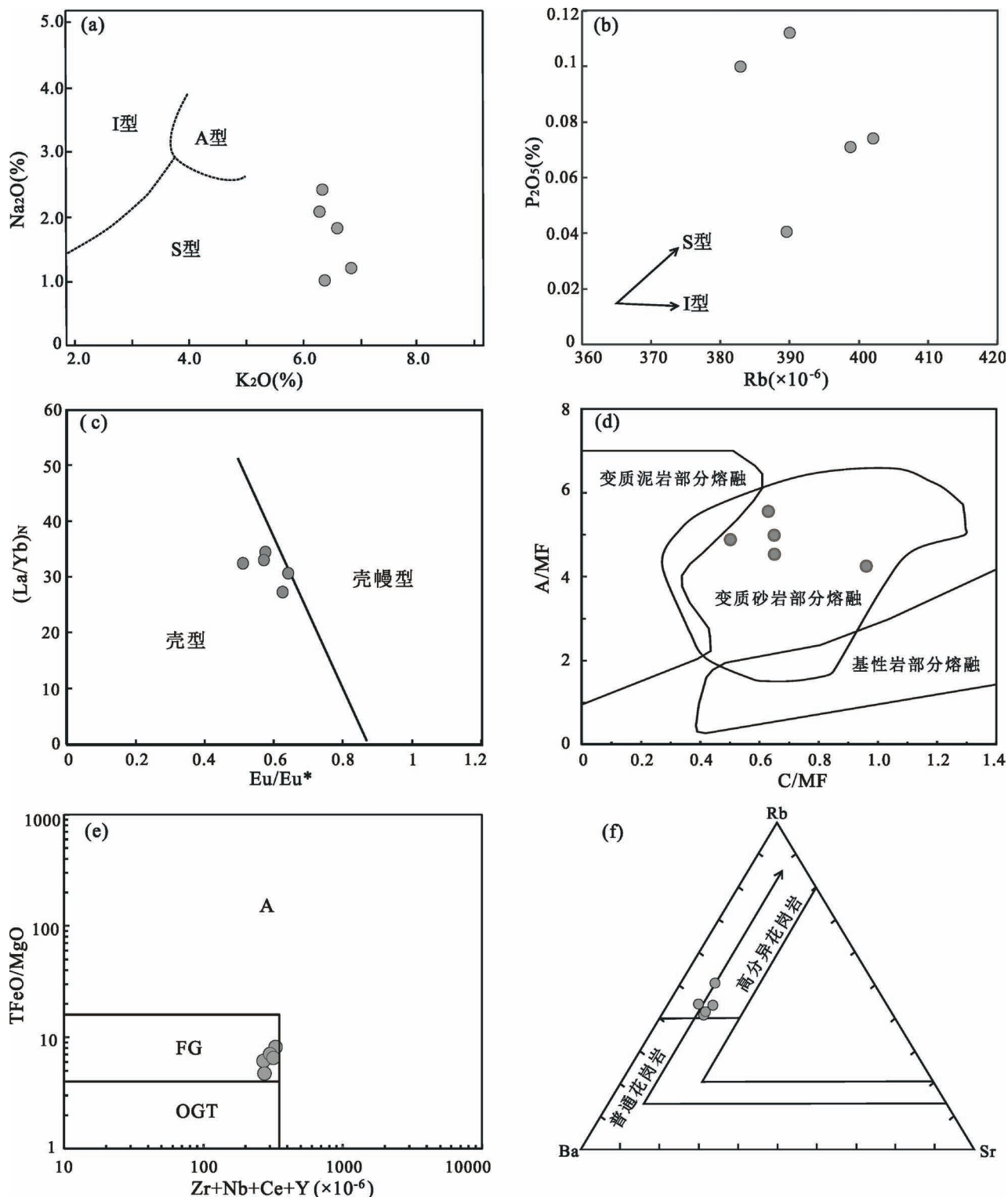


图 8 冈底斯成矿带西段则不吓矿床钾长花岗斑岩成因类型判别图解

Fig. 8 Geochemical classification diagrams of K-feldspar granite porphyries from the Zebuxia deposit in western Gangdese metallgenetic belt

OGT—未分异的 I、S、M 型花岗岩；FG—分异的长英质花岗岩

OGT—unfractionated I-, S- and M-type granite; FG—fractionated felsic granite

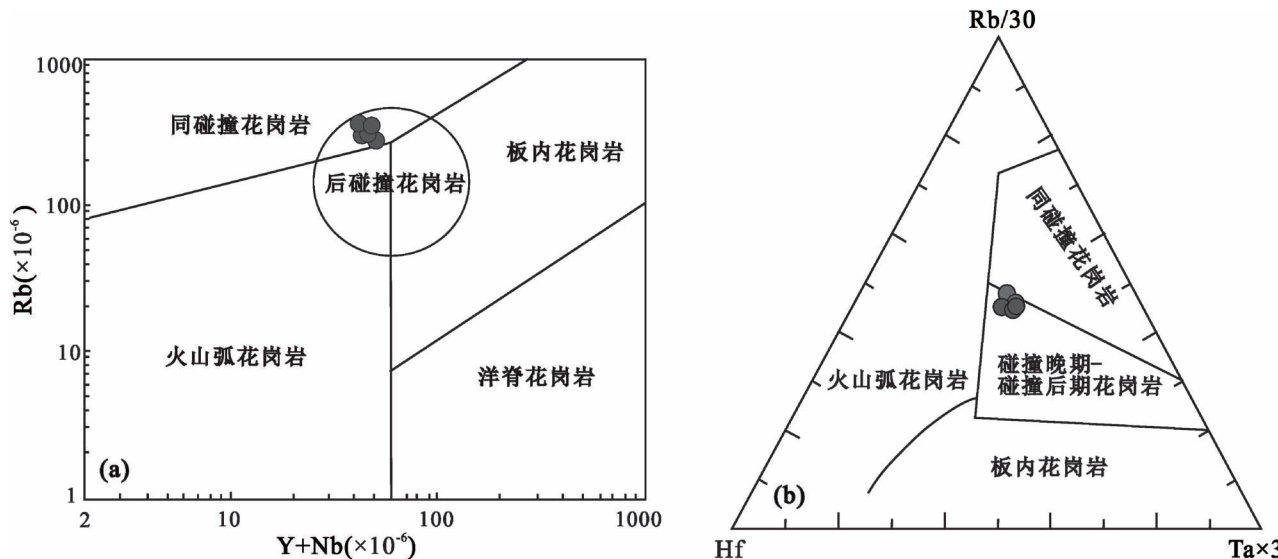


图 9 冈底斯成矿带西段则不吓矿床钾长花岗斑岩 ( $Y+Nb$ )— $Rb$  (a) (据 Pearce, 1996) 和 ( $Rb/30$ )— $Hf$ —( $Ta \times 3$ ) (b) (据 Hairs et al., 1986) 判别图解

Fig. 9 ( $Y+Nb$ )— $Rb$  diagram (a) (after Pearce et al., 1996) and ( $Rb/30$ )— $Hf$ —( $Ta \times 3$ ) diagram (b) (after Hairs et al., 1986) of K-feldspar granite porphyries from the Zebuxia deposit in western Gangdese metallgenetic belt

等, 2002); 则不吓钾长花岗斑岩为钾玄岩系列, 成岩较浅且存在表征高氧逸度的磁铁矿和富含挥发分的磷灰石(图 3e), 符合上述条件。另外, 则不吓矿区物化探特征反映其深部可能存在隐伏岩体, 地表出露的断裂构造很可能是岩浆侵入在顶部引爆形成的裂隙, 而各类斑岩脉为深部岩体向上延伸的分支(杜保峰等, 2019)。因此, 则不吓钾长花岗斑岩很有可能与铅锌矿体为一对同源分体(汪相等, 2022), 其侵位年龄可间接代表铅—锌矿化发生时间, 但其是否为成矿母岩还是仅仅提供成矿热量或部分成矿物质仍有待进一步研究确认。

冈底斯成矿带中新世成矿以斑岩型铜(—钼)矿化为主, 部分伴生同时期的矽卡岩型、热液脉型铅—锌矿化(李光明等, 2011; 赵晓燕等, 2013), 这些矿床在成岩—成矿年龄上具有高度的一致性, 集中形成于 18~12 Ma, 与前述大规模岩浆事件时代一致, 均为青藏高原经历了强烈碰撞挤压以及剪切走滑之后而进入地壳伸展阶段的产物(芮宗瑶等, 2004; 王立强等, 2014)。则不吓钾长花岗斑岩侵位年龄为 14 Ma 左右, 反映钾长花岗斑岩及相关铅—锌矿化系中新世岩浆活动的产物, 这与冈底斯带中新世大规模斑岩侵位时代和相关斑岩型铜(—钼)多金属矿化时代亦较一致(李光明等, 2011; 侯增谦等, 2012), 尤其相邻的朱诺铜矿区含矿花岗斑岩形

成年龄为 15.6 Ma(郑有业等, 2007), 因此则不吓铅锌矿床与冈底斯成矿带其它矿床很可能具有相同的成岩成矿环境, 应属于同一构造演化阶段产物。

## 5 结论

(1) 则不吓钾长花岗斑岩属钾玄岩系列, 岩石总体具高硅、富钾而贫镁特征, A/CNK 值介于 1.08~1.38 之间, 属强过铝质花岗岩; REE 具有较明显的中等负 Eu 异常, 总体呈现出向右倾斜的轻稀土富集模式; 微量元素富集 Rb、K、U、Th、Pb 等大离子亲石元素, 而 Ba、Sr 和 Nb、Ta、Ti、P 等高场强元素相对亏损。根据矿物组成和岩石地球化学特征, 表明其应属分异的 S 型花岗岩, 可能以壳源成分为主。

(2) 锆石 U-Pb 同位素年代学显示, 则不吓铅锌矿床钾长花岗斑岩形成年龄为  $14.18 \pm 0.15$  Ma, 系中新世岩浆活动的产物, 与印度—亚洲大陆碰撞后伸展背景下的引张构造有关, 且与冈底斯带中新世大规模斑岩侵位时代和相关斑岩型铜(—钼)矿化时代一致, 可能具有相同的成岩成矿环境, 应属于同一构造演化阶段产物。

(3) 则不吓铅—锌矿床位于西藏冈底斯中部驱龙—邦铺—朱诺斑岩铜—钼—铅—锌成矿亚带的西段, 且存在与铅锌矿化有关的岩浆活动, 这为在该成矿带中西段寻找到有工业价值的与斑岩有关的铅—

锌矿床提供了理论及实际依据,因此在后续找矿工作中,应该按照成矿系统的思想,注意在热液脉型铅锌矿体深部开展隐爆角砾岩型铅—锌银矿和斑岩型铜—钼—多金属矿的寻找。

**致谢:**野外地质调查及成文过程中得到河南省地质调查院的张彦启教授级高级工程师、董海敏工程师等的大力支持和指导,中国地质调查局天津地质调查中心耿建珍在实验过程中给予了帮助,同时审稿专家对论文提出了建设性意见,在此一并表示感谢!

## 参 考 文 献 / References

(The literature whose publishing year followed by a “&” is in Chinese with English abstract; The literature whose publishing year followed by a “#” is in Chinese without English abstract)

- 董旭舟,周振华,王润和,李进文,何姝. 2014. 内蒙古敖包吐铅锌矿床花岗岩类年代学及其地球化学特征. 矿床地质,33(2):323~338.
- 杜保峰,杨长青,李光耀,何凯,张荣臻,李滢琪. 2019. 西藏则不吓铅锌矿床地质、物化探特征及找矿前景. 地质与勘探,55(4):965~974.
- 费光春,温春齐,王成松,周雄,吴鹏宇,温泉,周玉. 2010. 西藏墨竹工卡县洞中拉花岗斑岩锆石SHRIMP U-Pb定年. 中国地质,37(2):470~476.
- 耿建珍,张健,李怀坤,李惠民,张永清,郝爽. 2012. 10 $\mu\text{m}$ 尺度锆石U-Pb年龄的LA-MC-ICP-MS测定. 地球学报,33(6):877~884.
- 侯增谦,莫宣学,杨志明,王安建,潘桂棠,曲晓明,聂凤军. 2006. 青藏高原碰撞造山带成矿作用:构造背景、时空分布和主要类型. 中国地质,33(3):340~351.
- 侯增谦,郑远川,杨志明,杨竹森. 2012. 大陆碰撞成矿作用:冈底斯新生代斑岩铜矿系统. 矿床地质,31(4):647~670.
- 黄瀚霄,张林奎,刘洪,李光明,黄勇,兰双双,吕梦鸿. 2019. 西藏冈底斯成矿带西段矿床类型、成矿作用和找矿方向. 地球科学,44(6):1876~1887.
- 黄勇,丁俊,李光明,戴婕,闫国强,王刚,刘晓峰. 2015. 西藏朱诺斑岩铜—钼—金矿区侵入岩锆石U-Pb年龄、Hf同位素组成及其成矿意义. 地质学报,89(1):99~108.
- 纪现华,孟祥金,杨竹森,张乾,田世洪,李振清,刘英超,于玉帅. 2014. 西藏纳如松多隐爆角砾岩型铅锌矿床绢云母Ar-Ar定年及其地质意义. 地质与勘探,50(2):281~290.
- 李光明,芮宗瑶. 2004. 西藏冈底斯成矿带斑岩铜矿的成岩成矿年龄. 大地构造与成矿学,28(2):165~170.
- 李光明,刘波,丁俊,潘桂棠,余宏全,朱弟成,王高明,芮宗瑶. 2011. 西藏冈底斯成矿带及邻区铜铁多金属矿成矿规律与成矿预测. 北京:地质出版社:1~270.
- 马旺,刘英超,杨竹森,李振清,赵晓燕,岳龙龙,唐波浪. 2020. 西藏列廷冈—勒青拉铅锌铁铜钼矿床硫化物Re-Os和Rb-Sr年龄及其地质意义. 矿床地质,39(1):80~96.
- 孟祥金,侯增谦,叶培盛,杨竹森,李振清,高永丰. 2007. 西藏冈底斯银多金属矿化带的基本特征与成矿远景分析. 矿床地质,26(2):153~162.
- 潘桂棠,丁俊,姚冬生. 2004. 青藏高原及邻区地质图(1:150万). 成都:成都地图出版社:1~133.
- 曲晓明,侯增谦,李佑国. 2002. S、Pb同位素对冈底斯斑岩铜矿带成矿物质来源和造山带物质循环的指示. 地质通报,21(11):768~776.
- 芮宗瑶,李光明,张立生,王龙生. 2004. 西藏斑岩铜矿对重大地质事件的响应. 地学前缘,11(1):145~152.
- 唐菊兴,王立强,郑文宝,钟康惠. 2014. 冈底斯成矿带东段矿床成矿规律及找矿预测. 地质学报,88(12):2545~2555.
- 唐菊兴,丁帅,孟展,胡吉月,高一鸣,谢富伟,李壮,袁梅,杨宗耀,陈国荣,李于海,杨洪钰,付燕刚. 2016. 西藏林子宗群火山岩中首次发现低硫化型浅成低温热液型矿床——以斯弄多银多金属矿为例. 地球学报,37(4):461~470.
- 王立强,唐菊兴,陈毓川,罗茂澄,冷秋锋,陈伟,王焕. 2011. 西藏邦铺钼(铜)矿床含矿二长花岗斑岩LA-ICP-MS锆石U-Pb定年及地质意义. 矿床地质,30(2):349~360.
- 王立强,唐菊兴,郑文宝,陈伟,林鑫,康浩然,罗茂澄. 2014. 西藏冈底斯成矿带东段主要钼多金属矿床成矿规律研究. 地质论评,60(2):363~379.
- 汪相,楼法生. 2022. 论岩浆热液矿床的成矿期——以南岭地区燕山期钨矿为例. 地质论评,68(2):507~530.
- 吴福元,刘小驰,纪伟强,王佳敏,杨雷. 2017. 高分异花岗岩的识别与研究. 中国科学(D辑),47(7):745~765.
- 吴元保,郑永飞. 2004. 锆石成因矿物学研究及其对U-Pb年龄解释的制约. 科学通报,49(16):1589~1604.
- 薛传东,骆少勇,宋玉才,杨志明,韩艳伟,黄琴辉,李敬,魏英爱. 2010. 滇西北中甸陆家村石英二长斑岩的锆石SHRIMP定年及其意义. 岩石学报,26(6):1845~1855.
- 应立娟,王登红,唐菊兴,畅哲生,屈文俊,郑文宝,王焕. 2010. 西藏墨竹工卡县甲玛铜多金属矿不同矿石中辉钼矿Re-Os同位素定年及其成矿意义. 地质学报,84(8):1165~1173.
- 臧文栓,孟祥金,杨竹森,叶培胜. 2007. 西藏冈底斯成矿带铅锌银矿床的S、Pb同位素组成及其地质意义. 地质通报,26(10):1393~1397.
- 张松,郑远川,黄克贤,李为,孙清钟,李秋耘,付强,梁维. 2012. 西藏努日砂卡岩型铜钨钼矿辉钼矿Re-Os定年及其地质意义. 矿床地质,31(2):337~346.
- 赵晓燕,杨竹森,刘英超,纪现华,费凡,徐玉涛. 2013. 西藏夏垅铅锌银矿床绢云母<sup>40</sup>Ar/<sup>39</sup>Ar年龄及其地质意义. 矿床地质,32(5):963~971.
- 赵振华,熊小林,王强,包志伟,张玉泉,谢应雯,任双奎. 2002. 我国富碱火成岩及有关的大型—超大型金铜矿床成矿作用. 中国科学(D辑),32(增刊):1~10.
- 赵振华,熊小林,王强,乔玉楼. 2008. 钨与钽的某些地球化学问题. 地球化学,37(4):304~320.
- 赵志丹,莫宣学,Nomade S.,Renne P R,周肃,董国臣,王亮亮,朱弟成,廖忠礼. 2006. 青藏高原拉萨地块碰撞后超钾质岩石的时空分布及其意义. 岩石学报,22(4):787~794.
- 郑有业,张刚阳,许荣科,高顺宝,庞迎春,曹亮,杜安道,石玉若. 2007. 西藏冈底斯朱诺斑岩铜矿床成岩成矿时代约束. 科学通报,52(21):2542~2548.
- Alther R, Holl A, Hegner E, Langer C, Kreuzer H. 2000. High-potassium, calc-alkaline I-type plutonism in the European Variscides: Northern Vosges (France) and northern Schwarzwald (Germany). Lithos,50:51~73.
- Andersen T. 2002. Correction of common lead in U-Pb analyses that do not report <sup>204</sup>Pb. Chemical Geology,192: 59~79.
- Bouseily A M and Sokkary A A. 1975. The relation between Rb, Ba and Sr in granitic rocks. Chemical Geology,16:207~219.
- Barbarin. 1999. A review of the relationships between granitoid type, their origins and their geodynamic environments. Lithos,46:605~

- 626.
- Belousova E A, Suzanne G W, Fisher Y. 2002. Igneous zircon: Trace element composition as an indicator of source rock type. Contribution to Mineralogy and Petrology, 143:602~622.
- Chappell B W and White A J R. 1992. I- and S-type granites in the Lachlan Fold Belt. Transactions of the Royal Society of Edinburgh. Earth sciences, 83:1~26.
- Dong Xuzhou, Zhou Zhenhua, Wang Runhe, Li Jinwen, He Shu. 2014&. Geochronology and geochemistry of granite in Aobaotu Pb—Zn deposit, Inner Mongolia. Mineral Deposits, 33(2):323~338.
- Du Baofeng, Yang Changqing, Li Guangyao, He Kai, Zhang Rongzhen, Li Yingqi. 2019&. Analysis of geological, gophysical and geochemical characteristics and prospecting potentiality of the Zebuxia Pb—Zn deposit, Tibet. Geology and Exploration, 55(4):965~974.
- Fei Guangchun, Wen Chunqi, Wang Chengsong, Zhou Xiong, Wu Pengyu, Wen Quan, Zhou Yu. 2010&. Zircon SHRIMP U-Pb age of porphyry granite in the Dongzhongla lead—zinc deposit, Maizhokunggar County, Tibet. Geology in China, 37(2):470~476.
- Forster H J, Tischendorf G, Trumbull R B. 1997. An evaluation of the Rb vs. (Y+ Nb) discrimination diagram to infer tectonicsetting of silicic igneous rocks. Lithos, 40:261~293.
- Geng Jianzhen, Zhang Jian, Li Huaikun, Li Huimin, Zhang Yongqing, Hao Shuang. 2012&. Ten micron-sized zircon U-Pb dating using LA-MC-ICP-MS. Acta Geoscientica Sinica, 33(6):877~884.
- Harris N B W, Pearce J A, Tindle A G. 1986. Geochemicalcharacteristics of collision zone magmatism. Geological Society of London, 19:67~81.
- Hoskin P W O and Black L P. 2000. Metamorphic zircon formation by solid state recrystallization of protolith igneous zircon. Journal of Metamorphic Geology, 18:423~439.
- Hoskin P W O and Schaltegger U. 2003. The composition of zircon and igneous and metamorphic petrogenesis. Reviews in Mineralogy and Geochemistry, 53:27~62.
- Hou Zengqian, Gao Yongfeng, Qu Xiaoming, Rui Zongyao, Mo Xuanxue. 2004. Origin of adakitic intrusives generated during Mid-Miocene east—west extension in southern Tibet. Earth and Planetary Science Letters, 220:139~155.
- Hou Zengqian, Mo Xuanxue, Yang Zhiming, Wang Anjian, Pan Guitang, Qu Xiaoming, Nie Fengjun. 2006&. Metallogenesis in the collisional orogen of the Qinghai—Tibet Plateau: Tectonic setting, tempo—spatial distribution and ore deposit types. Geology in China, 33(3):340~351.
- Hou Zengqian, Yang Zhiming, Qu Xiaoming, Meng Xiangjin, Li Zhengqing, Beaudoin G, Rui Zongyao, Gao Yongfeng, Khin Z. 2009. The Miocene Gangdese porphyry copper belt generated during post-collisional extension in the Tibetan Orogen. Ore Geology Review, 36:25~51.
- Hou Zengqian, Zheng Yuanchuan, Yang Zhiming, Yang Zhugen. 2012&. Metallogenesis of continental collision setting: Part I. Gangdese Cenozoic porphyry Cu—Mo systems in Tibet. Mineral Deposits, 31(4):647~670.
- Huang Hanxiao, Zhang Linkui, Liu Hong, Li Guangming, Huang Yong, Lan Shuangshuang, Lü Menghong. 2019&. Major Types, Mineralization and potential prospecting areas in western section of the Gangdese metallogenic belt, Tibet. Earth Science, 44(6):1876~1887.
- Huang Yong, Ding Jun, Li Guangming, Dai Jie, Yan Guoqinag, Wang Gang, Liu Xiaofeng. 2015&. U-Pb dating, Hf isotopic characteristics of zircons from intrusions in the Zhunuo porphyry Cu—Mo—Au deposit and its mineralization significance. Acta Geologica Sinica, 89(1):99~108.
- Ji Xianhua, Meng Xiangjin, Yang Zhugen, Zhang Qian, Tian Shihong, Li Zhenqing, Liu Yingchao, Yu Yushuai. 2014&. The Ar-Ar geochronology of sericite from the cryptoexplosive breccia type Pb—Zn deposit in Narusongduo, Tibet and its geological significance. Geology and Exploration, 50(2): 281~ 290.
- Kelley K D and Ludingtons. 2002. Cripple Creek and other alkaline related gold deposits in the southern Rocky Mountains, USA: influence of regional tectonics. Mineralium Deposita, 37(1):38~60.
- Li Guangming and Rui Zongyao. 2004&. Diagenetic and mineralization ages for theporphyry copper deposits in the Gangdese metallogenic belt, southern Tibet. Geotectonica et Metallogenica, 28(2):165~170.
- Li Guangming, Liu Bo, Ding Jun, Feng Chengyou, Qu Wenjun. 2006&. Early Himalayan mineralization on the southern margin of the Gangdese metallogenic belt, Tibet, China; Evidence from Re-Os ages of the Chongmuda skarn-type Cu—Au deposit. Geological Bulletin of China, 25(12):1481~1486.
- Li Guangming, Liu Bo, Ding Jun, Pan Guitang, She Hongquan, Zhu Dichen, Wang Gaoming, Rui Zongyao. 2011#. Metallogenic Regularities and Prospecting Prediction of Iron Copper Polymetallic Deposits in Gangdese Metallogenic Belt and Its Neighboring Area, Tibet. Beijing:Geological Publishing House:1~270.
- Maheo G, Guillot S, Blichert-Tofa J, Rolland Y, Pecher A. 2002. A slab breakoff model for the Neogene theamal evolution of South Karakorum and South Tibet. Earth Science Letter, 195:45~48.
- Ma Wang, Liu Yingchao, Yang Zhugen, Li Zhenqing, Zhao Xiaoyan, Yue Longlong, Tang Bolang. 2020&. Sulfide Re-Os and Rb-Sr ages of Lietinggang—Leqingla Pb—Zn—Fe—Cu—Mo deposit in Tibet and its geological significance. Mineral Deposits, 39(1):80~96.
- Meng Xiangjin, Hou Zengqian, Ye Peisheng, Yang Zhugen, Li Zhenqing, Gao Yongfeng. 2007&. Characteristics and ore potentiality of Gangdese silver—polymetallic mineralization belt in Tibet. Mineral Deposits, 26(3):153~162.
- Miller C, Schuater R, Klotzli U, Frank N, Pertacher F. 1999. Post-collisional potassic and ultrapotassic magmatism in SW Tebet: Geochemical and Sr—Nd—Pb—O isotopic constraints for mantle source characteristics and petrogenesis. Journal of Petrology, 40: 1399~1424.
- Moeller A, Brien P J, Kennedy A. 2003. Linking growth episodes of zircon and metamorphic textures to zircon chemistry: an example from the ultrahigh-temperature granulites of Rogaland, SW Norway. Geological Society, London, Special Publications, 220:65~81.
- Pan Guitang, Ding Jun, Yao Dongsheng. 2004#. Geological Map of the Tibetan Plateau and Adjacent Regions (1: 1500000). Chengdu: Chengdu Map Publishing House:1~133.
- Pearce J A. 1996. Source and settings of granitic rocks. Episodes, 19: 120~125.
- Qu Xiaoming, Hou Zengqian, Li Youguo. 2002&. Implications of S and Pb isotopic compositions of the Gangdese porphyry copper belt for the ore-forming material source and material recycling with in the orogenic belt. Geological Bullet in of China, 21(11):768~776.
- Rui Zongyao, Li Guangming, Zhang Li Sheng, Wang Longsheng. 2004&. The response of porphyry copper deposits important geological events in Tibet. Earth Science Frontiers, 11(1):145~152.

- Sillitoe R H. 1997. Charateristics and controls of the largest porphyry copper—gold and epithermal gold deposits in the circum Pacific region. Australian Journal of Earth Sciences, 44(3) :373~388.
- Sun S S and McDonough W F. 1989. Chemical and isotopic systematics of oceanic basalts: implications for mantle composition and processes. Geological Society, London, Special Publications, 42:313 ~345.
- Sylvester P J. 1998. Post-collisional strongly peraluminous granites. Lithos, 45:29~44.
- Tang Juxing, Wang Liqiang, Zheng Wenbao, Zhong Kanghui. 2014&. Ore deposits metallogenetic regularities and prospecting in the eastern section of Gangdese metallogenetic belt. Acta Geologica Sinica, 88 ( 12 ) : 2545~2555.
- Tang Juxing, Ding Shuai, Meng Zhan, Gao Yiming, Xie Fuwei, Li Zhuang, Yuan Mei, Yang Zongyao, Chen Guorong, Li Yuhai, Yang Hongyu, Fu Yangang. 2016&. The first discovery of the low sulfidation epithermal deposit in Linzizong volcanics, Tibet: A case study of the Sinogduo Ag polymetallic deposit. Acta Geoscientica Sinica, 37 ( 4 ) :461~470.
- Wang Xiang and Lou Fasheng. 2022&. On the ore-forming period of magmatic—hydrothermal deposits——A case study of the Yanshanian tungsten deposits in the Nanling Range. Geological Review, 68(2) :507~530.
- Whalen J B, Currie K L, Chappell B W. 1987. A-type granites: Geochemical characteristics, discrimination and petrogenesis. Contribution to Mineralogy and Petrology, 95:407~419.
- Wu Fuyuan, Liu Xiaochi, Ji Weiqiang, Wang Jiamin, Yang Lei. 2017&. Highly fractionated granites: Recognition and research. Science China Earth Sciences, 47 ( 7 ) :745~765.
- Wu Yuanbao and Zheng Yongfei. 2004#. Zircon genesis mineralogy and its restriction for U-Pb age. Chinese Science Bulletin, 49 ( 16 ) : 1589~1604.
- Xue Chuandong, Luo Shaoyong, Song Yucai, Yang Zhiming, Han Yanwei, Huang Qinhui, Li Jing, Wei Yingai. 2010&. Zircon SHRIMP U-Pb dating and its geological significance of Lujiacun quartz-monzonite porphyry in Shangri-la County, northwestern Yunnan Province, China. Acta Petrologica Sinica, 26 ( 6 ) :1845~1855.
- Ying Lijuan, Wang Denghong, Tang Juxing, Chang Zhesheng, Qu Wenjun, Zheng Wenbao, Wan Huan. 2010&. Re-Os dating of molybdenite from the Jiama copper polymetallic deposit in Tibet and its metallogenetic significance. Acta Geologic Sinica, 84 ( 8 ) : 1165 ~ 1173.
- Zang Wenshuan, Meng Xiangjin, Yang Zhusen, Ye Peisheng. 2007&. Sulfur and lead isotopic compositions of lead—zinc—silver deposits in the Gangdise metallogenetic belt, Tibet, China, and its geological significance. Geological Bulletin of China, 26 ( 10 ) :1393~1397.
- Zhang Song, Zheng Yuanchuan, Huang Kexian, Li Wei, Sun Qinzhong, Li Qiuyun, Fu Qiang, Liang Wei. 2012&. Re-Os dating of molybdenite from Nuri Cu—W—Mo deposit and its geological significance. Mineral Deposits, 31 ( 2 ) :337~346.
- Zhao Xiaoyan, Yang Zhusen, Liu Yingchao, Ji Xianhua, Fei Fan, Xu Yutao. 2013&.  $^{40}\text{Ar}/^{39}\text{Ar}$  dating of sericite from Xialong Pb—Zn—Ag deposit and its geological significance. Mineral Deposits, 32 ( 5 ) :963~971.
- Zhao Zhenhua, Xiong Xiaolin, Wang Qiang, Bao Zhiwei, Zhang Yuquan , Xie Yingwen, Ren Shuangkui. 2002#. Alkali-rich igneous rocks and Ore-forming effect of related large—super-large gold—copper deposits in China. Science in China ( Series D ), 32 ( Supp ) :1~10.
- Zhao Zhenhua, Xiong Xiaolin, Wang Qiang, Qiao Yulou. 2008&. Some aspects on geochemistry of Nb and Ta. Geochemica, 37 ( 4 ) :304 ~ 320.
- Zhao Zhidan, Mo Xuanxue, Nomade S, Renen P R, Zhou Su, Dong Guochen, Wang Liangliang, Zhu Dicheng, Liao Zhongli. 2006&. Post-collisional ultrapotassic rocks in Lhasa Block, Tibestan Paetau: spatial and temporal distribution and its implications. Acta Petrologica Sinica, 22 ( 4 ) :787~794.
- Zheng Youye, Zhang Gangyang, Xu Rongke, Gao Shunbao, Pang Yingchun, Cao Liang, Du Andao, Shi Yuruo. 2007#. Restriction for diagenesis—mineralization ages of the Gangdese metallogenetic belt, Tibet. Chinese Science Bulletin, 52 ( 21 ) :2542~2548.

## Geochronology, geochemistry and geological significance of the K-feldspar granite porphyry from Zebuxia Pb—Zn deposit, Xizang (Tibet)

DU Baofeng<sup>1,2)</sup>, HE Kai<sup>2)</sup>, YANG Changqing<sup>2)</sup>, CHAI Zhichao<sup>2)</sup>, LU Peiqing<sup>2)</sup>, GENG Aibin<sup>2)</sup>  
 1) China University of Geosciences (Beijing), Beijing, 100083;

2) Henan Institute of Geological Survey, Henan Key Laboratory of Metal Mineral Mineralization Geological Processes and Resource Utilization, Zhengzhou, 450001

**Objectives:** The Zebuxia Pb—Zn deposit is located in the western of Gangdese porphyry Cu—Mo—Polymetallic metallogenetic belt, Xizang (Tibet), which occurs lots of K-feldspar granite porphyry. In order to find out formation age and genetic types of the K-feldspar granite porphyry, further discuss diagenetic environment and the relationship with Pb—Zn mineralization.

**Methods:** Detailed geological survey, LA-MC-ICP-MS zircon U-Pb dating and the whole-rock geochemical analysis of K-feldspar granite porphyry.

**Results:** Zircon U-Pb geochronology results show that the K-feldspar granite porphyry was formed in  $14.18 \pm 0.15$  Ma pertain to magmatic products of the Miocene. Major elements of the K-feldspar granite porphyries have characteristics of enrichment silica and alkali, depleted magnesium, A/CNK ranges from between 1.08 to 1.38.

Rare earth elements have the right-leaning pattern of the LREE enrichment and medium negative Eu abnormality. Trace elements are rich in Rb, Th, U, K and Pb, but which are poor in Ba, Sr and HFSE, such as Nb, Ta, P and Ti.

**Conclusions:** K-feldspar granite porphyries have the differentiation characteristics of S-type granite. The K-feldspar granite porphyries were probably formed in post-collision extensional setting background followed the Indian—Asian continental collision, and consistent with the epoch of the massive porphyry emplacement period and associated porphyry copper (molybdenum) mineralization of Gangdise metallogenic belt in the Miocene, namely they may have the same diagenesis and mineralization environment. In addition, it provides theoretical and practical basis for prospecting porphyry-related Pb—Zn deposits in the western part of the Gangdise metallogenic belt.

**Keywords:** U-Pb geochronology; geochemical; Miocene; K-feldspar granite porphyry; Zebuxia; Gangdese metallogenic belt

**Acknowledgements:** Supported by China Geological Survey Program (No. 121201010000150014-17)

**The first author:** DU Baofeng, male, born in 1985, doctoral student, senior engineer, is mainly engaged in mineral deposits and exploration; Email: dubaofeng517@163.com

**Manuscript** received on: 2022-01-21; Accepted on: 2022-06-08; Network published on: 2022-06-20

**Doi:** 10.16509/j.georeview.2022.06.115

**Edited by:** ZHANG Yuxu

